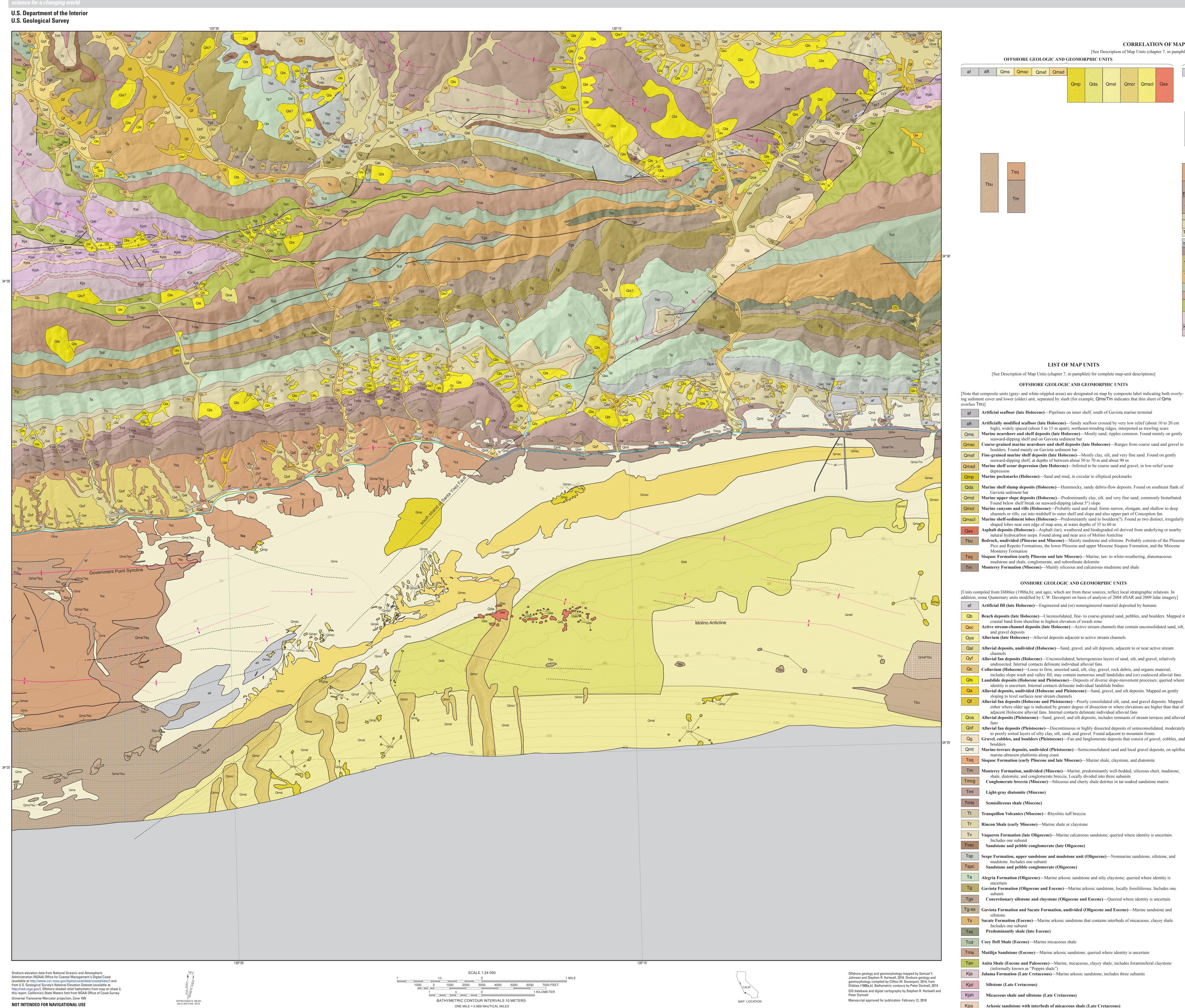
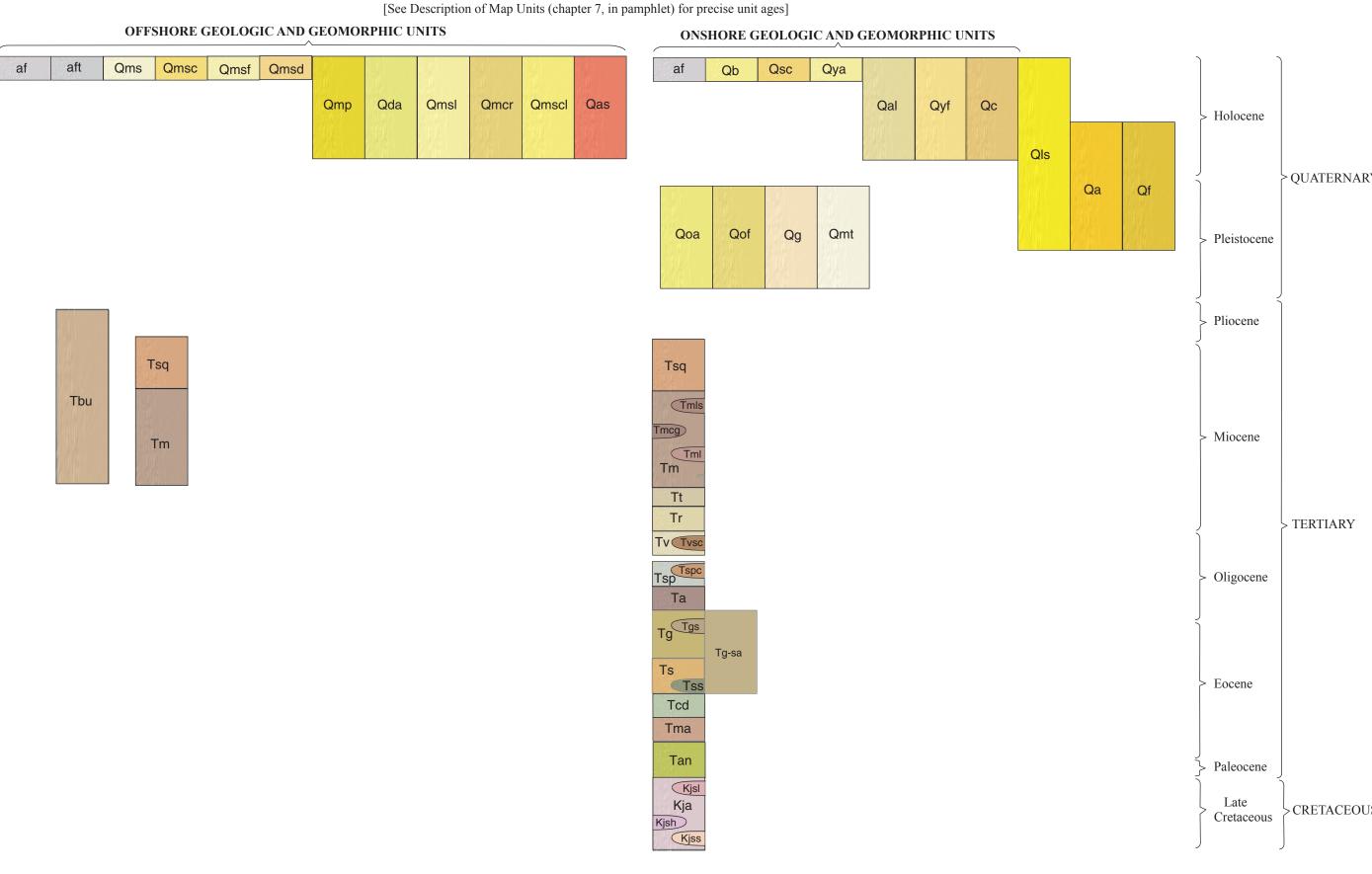
Pamphlet accompanies map





**CORRELATION OF MAP UNITS** 

LIST OF MAP UNITS

[See Description of Map Units (chapter 7, in pamphlet) for complete map-unit descriptions]

OFFSHORE GEOLOGIC AND GEOMORPHIC UNITS

Artificially modified seafloor (late Holocene)—Sandy seafloor crossed by very low relief (about 10 to 20 cm

high), widely spaced (about 5 to 15 m apart), northeast-trending ridges, interpreted as trawling scars

Marine nearshore and shelf deposits (late Holocene)—Mostly sand; ripples common. Found mainly on gently

Coarse-grained marine nearshore and shelf deposits (late Holocene)—Ranges from coarse sand and gravel to

**Fine-grained marine shelf deposits (late Holocene)**—Mostly clay, silt, and very fine sand. Found on gently

Marine shelf slump deposits (Holocene)—Hummocky, sandy debris-flow deposits. Found on southeast flank of

Marine upper slope deposits (Holocene)—Predominantly clay, silt, and very fine sand; commonly bioturbated.

Marine shelf-sediment lobes (Holocene)—Predominantly sand to boulders(?). Found as two distinct, irregularly

**Asphalt deposits (Holocene)**—Asphalt (tar); weathered and biodegraded oil derived from underlying or nearby

Pico and Repetto Formations, the lower Pliocene and upper Miocene Sisquoc Formation, and the Miocene

Marine canyons and rills (Holocene)—Probably sand and mud; forms narrow, elongate, and shallow to deep

channels or rills; cut into midshelf to outer shelf and slope and also upper part of Conception fan

Bedrock, undivided (Pliocene and Miocene)—Mainly mudstone and siltstone. Probably consists of the Pliocene

Sisquoc Formation (early Pliocene and late Miocene)—Marine, tan- to white-weathering, diatomaceous

ONSHORE GEOLOGIC AND GEOMORPHIC UNITS

Qb Beach deposits (late Holocene)—Unconsolidated, fine- to coarse-grained sand, pebbles, and boulders. Mapped in

Qal Alluvial deposits, undivided (Holocene)—Sand, gravel, and silt deposits, adjacent to or near active stream

Alluvial fan deposits (Holocene)—Unconsolidated, heterogeneous layers of sand, silt, and gravel; relatively

**S** Landslide deposits (Holocene and Pleistocene)—Deposits of diverse slope-movement processes; queried where

Alluvial fan deposits (Holocene and Pleistocene)—Poorly consolidated silt, sand, and gravel deposits. Mapped

Alluvial deposits (Pleistocene)—Sand, gravel, and silt deposits; includes remnants of stream terraces and alluvial

to poorly sorted layers of silty clay, silt, sand, and gravel. Found adjacent to mountain fronts

Qmt Marine-terrace deposits, undivided (Pleistocene)—Semiconsolidated sand and local gravel deposits, on uplifted

Conglomerate breccia (Miocene)—Siliceous and cherty shale detritus in tar-soaked sandstone matrix

Gaviota Formation (Oligocene and Eocene)—Marine arkosic sandstone, locally fossiliferous. Includes one

Ts Sacate Formation (Eocene)—Marine arkosic sandstone that contains interbeds of micaceous, clayey shale.

Tan Anita Shale (Eocene and Paleocene)—Marine, micaceous, clayey shale; includes foraminiferal claystone

Kja Jalama Formation (Late Cretaceous)—Marine arkosic sandstone; includes three subunits

Concretionary siltstone and claystone (Oligocene and Eocene)—Queried where identity is uncertain

Alluvial fan deposits (Pleistocene)—Discontinuous or highly dissected deposits of semiconsolidated, moderately

**Gravel, cobbles, and boulders (Pleistocene)**—Fan and fanglomerate deposits that consist of gravel, cobbles, and

includes slope wash and valley fill; may contain numerous small landslides and (or) coalesced alluvial fans

either where older age is indicated by greater degree of dissection or where elevations are higher than that of

**Colluvium (Holocene)**—Loose to firm, unsorted sand, silt, clay, gravel, rock debris, and organic material;

Alluvial deposits, undivided (Holocene and Pleistocene)—Sand, gravel, and silt deposits. Mapped on gently

adjacent Holocene alluvial fans. Internal contacts delineate individual alluvial fans

Tsq Sisquoc Formation (early Pliocene and late Miocene)—Marine shale, claystone, and diatomite

shale, diatomite, and conglomerate breccia. Locally divided into three subunits

Active stream-channel deposits (late Holocene)—Active stream channels that contain unconsolidated sand, silt,

Marine shelf scour depression (late Holocene)—Inferred to be coarse sand and gravel, in low-relief scour

Artificial seafloor (late Holocene)—Pipelines on inner shelf, south of Gaviota marine terminal

seaward-dipping shelf, at depths of between about 50 to 70 m and about 90 m

Marine pockmarks (Holocene)—Sand and mud, in circular to elliptical pockmarks

shaped lobes near east edge of map area, at water depths of 35 to 60 m

natural hydrocarbon seeps. Found along and near axis of Molino Anticline

Found below shelf break on seaward-dipping (about 5°) slope

mudstone and shale, conglomerate, and subordinate dolomite

coastal band from shoreline to highest elevation of swash zone

Qya Alluvium (late Holocene)—Alluvial deposits adjacent to active stream channels

undissected. Internal contacts delineate individual alluvial fans

sloping to level surfaces near stream channels

marine-abrasion platforms along coast

Tr Rincon Shale (early Miocene)—Marine shale or claystone

VSC Sandstone and pebble conglomerate (late Oligocene)

Sandstone and pebble conglomerate (Oligocene)

mudstone. Includes one subunit

Includes one subunit

Includes one subunit

Kisl Siltstone (Late Cretaceous)

Predominantly shale (late Eocene)

(informally known as "Poppin shale")

Micaceous shale and siltstone (Late Cretaceous)

Kjss Arkosic sandstone with interbeds of micaceous shale (Late Cretaceous)

identity is uncertain. Internal contacts delineate individual landslide bodies

Tm Monterey Formation (Miocene)—Mainly siliceous and calcareous mudstone and shale

af Artificial fill (late Holocene)—Engineered and (or) nonengineered material deposited by humans

seaward-dipping shelf and on Gaviota sediment bar

boulders. Found mainly on Gaviota sediment bar

**EXPLANATION OF MAP SYMBOLS** ——— Contact—Solid where location is certain or well located, dashed where location is approximate or inferred **Fault**—Solid where location is certain, dashed where location is inferred, dotted where location is concealed, queried where uncertain Folds—Solid where location is certain, dashed where location is inferred, dotted where location is concealed \_\_\_\_\_ Approximate modern shoreline—From National Oceanic and Atmospheric Administration's Shoreline Data Explorer (National Geodetic Survey, 2016) 3-nautical-mile limit of California's State Waters **Area of "no data"**—Areas beyond 3-nautical-mile limit of California's State Waters were not mapped as part of California Seafloor Mapping Program

**DISCUSSION** Marine geology and geomorphology were mapped in the Offshore of Gaviota map area from the shoreline to the 3-nautical-mile limit of California's State Waters. The location of the shoreline, which is from the National Oceanic and Atmospheric Administration's (NOAA's) Shoreline Data Explorer, is based on their analysis of lidar imagery (National Geodetic Survey, 2016). Offshore geologic units were delineated on the basis of integrated analyses of adjacent onshore geology with multibeam bathymetry and backscatter imagery (sheets 1, 2, 3), seafloor-sediment and rock samples (Reid and others, 2006), digital camera and video imagery (Golden and Cochrane, 2013), and high-resolution seismic-reflection profiles (sheet 7). Bathymetric lidar and aerial photographs taken in multiple years were used to map the nearshore area (0 to 10 m water depth) and to link the offshore and onshore geology.

The onshore geology was compiled from Dibblee (1988a,b); unit ages, which are derived from these sources, reflect local stratigraphic relations. In addition, some Quaternary units were modified by C.W. Davenport on the basis of analysis of 2004 if SAR and 2009 lidar imagery. The offshore part of the map area largely consists of a narrow (4- to 5-km-wide), gently (about 1° to 1.5°) offshoredipping shelf underlain by Neogene bedrock, as well as Holocene sediments that are derived primarily from Cañada de la Gaviota and smaller coastal watersheds that drain the Santa Ynez Mountains (see fig. 1–2, in pamphlet). Holocene nearshore and shelf deposits are primarily sand (unit Qms). Coarser grained sediments (unit Qmsc) are found mainly along the Gaviota sediment bar, a prominent bathymetric feature that extends southwestward for about 9 km from the mouth of Cañada de la Gaviota to the shelf break. The Gaviota sediment bar, which faces southeast, is as wide as 2 km and has a relatively flat (about 1.4°) top that extends to water depths of 60 m. The steep (as much as 5°) bar front, which formed by advancing clinoforms (see fig. 5 on sheet 7), is bounded by an apron of coalescing, hummocky debris-flow lobes (unit Qda). Coarser grained sediment also is present in the eastern part of a small scour depression (unit Qmsd) found along the west edge of the map

area, at a water depth of about 35 m. Sandy seafloor (unit aft) that is crossed by very low relief (about 10 to 20 cm high),

widely spaced (about 5 to 15 m apart), northeast-trending ridges is found in two areas (827,209 and 289,593 m<sup>2</sup>) about 3.5 km

south of the Gaviota shoreline, in water depths of about 40 to 55 m; the morphology of these ridges suggests that they were formed by fishing trawls. Two subtle sediment lobes (unit Qmscl) are mapped near the east edge of the map area on the basis of their high backscatter and positive seafloor relief. These lobes, which occupy 257,490 and 92,932 m<sup>2</sup>, are found about 1,080 to 2,100 m offshore, in water depths of 35 to 55 m. The lobes are located offshore of the mouths of steep coastal watersheds, and they have been interpreted as the deposits of debris flows or hyperpycnal flows, or a combination of these processes (Warrick and others, 2013; Steel and others, 2015). Preliminary ages (Steel and others, 2015) on similar features to the east indicate that they may have formed as early as 8,500 years ago when sea level was significantly lower (Steel and others, 2015). Finer grained sediment—the very fine sand, silt, and clay of unit Qmsf—is mapped primarily in the eastern part of the map area, between depths of about 60 m and the shelf break. The boundary between units Qms and Qmsf is based on observations and extrapolation from sparse sediment sampling (for example, Reid and others, 2006) and camera ground-truth surveying (Golden and Cochrane, 2013). Thus, the boundary between units Qms and Qmsf should be considered transitional and approximate and is expected to shift as a result of seasonal- to annual- to decadal-scale cycles in wave climate, sediment

supply, and sediment transport. Fine-grained deposits similar to unit Qmsf also are found below the shelf break on the upper slope, at water depths greater than 90 m, where they are mapped as a separate unit (unit Qmsl) on the basis of their location and geomorphology. Both the shelf break and the distal part of the Gaviota sediment bar are incised by narrow rills and three large (150- to 300-m-wide) channels (collectively mapped as unit Qmcr) that have been referred to either as "the Gaviota Canyons" (Fischer and Cherven, 1998) or as "Drake Canyon," "Sacate Canyon," and "Alegria Canyon" (Eichhubl and others, 2002). East of the south strand of the Santa Ynez Fault, bedrock exposures along the shoreline and on the inner shelf consist of

siliceous and calcareous mudstone and shale of the Miocene Monterey Formation (unit Tm). West of this fault strand, bedrock

outcrops in the nearshore and on the shelf consist primarily of marine shale, claystone, and diatomite of the upper Miocene

and lower Pliocene Sisquoc Formation (unit Tsq). Seafloor outcrops of units Tm and Tsq both commonly have a "ribbed" appearance, reflecting the differential erosion of variably resistant interbeds. Because of the lack of sampling and their relative lack of distinctive seafloor morphology, some seafloor bedrock outcrops on the outer shelf cannot be confidently assigned to either unit Tm or unit Tsq; these areas are mapped as the undivided Tertiary bedrock unit (Tbu). The Santa Barbara Channel region is a mature hydrocarbon province that has a long history of petroleum exploration and production (Kunitomi and others, 1998). The Offshore of Gaviota map area includes the western part of the Molino offshore gas field, as well as the Gaviota and Caliente offshore gas fields and the Alegria and Cuarta offshore oil fields (Yerkes and others, 1969). Seafloor geomorphic features associated with petroleum seepage include fields of dense pockmarks (unit Qmp), asphalt mounds (unit Qas), carbonate mats, and mud volcanoes (see, for example, Keller and others, 2007). The pockmarks in the map area are predominantly grouped or, less commonly, solitary; are circular to elliptical; range in size from 50 to 150 m along their long axis; typically are 20 to 40 cm deep; and commonly have a central cone as much as 150 cm high. The largest field of pockmarks (709,384 m<sup>2</sup>) is along the trace of the south strand of the Santa Ynez Fault, along which fractured bedrock may provide a conduit for seepage. Asphalt mounds in the map area are found along and near the crest of

calculated a composite volume of asphalt in the Gaviota area of 4.5×10<sup>5</sup> m<sup>3</sup>. Offshore pipelines, which are associated with offshore oil and gas development, are mapped as unit af. Neogene strata are deformed in a fold belt that, on a regional scale, is located within a large, east-west-striking, southdipping homocline that extends from the south flank of the Santa Ynez Mountains into the offshore. Nearby regional cross sections (Redin and others, 2005) and industry seismic-reflection profiles (see fig. 6 on sheet 7; see also, Sorlien and Nicholson, 2015) showed that the homocline formed above the blind Pitas Point–North Channel Fault system, which in the offshore extends westward for more than 100 km, from Pitas Point (10 km northwest of Ventura) to beyond Gaviota and Point Conception (see fig. 1–3, in pamphlet). South of Gaviota, the tip of the Pitas Point–North Channel Fault is inferred to be buried beneath the slope, about 10 km offshore, to a depth of about 2 to 3 km below sea level. The southwest-striking south strand of the Santa Ynez Fault, as mapped onshore by Dibblee (1988b), is unique among

Santa Barbara fold-belt structures in that it obliquely crosses the Santa Ynez Mountains and the dominant east-west-trending

the Molino Anticline where they generally are less than 4 m high and less than 40 m in diameter (Lorenson and others, 2014);

Draut and others (2009) noted that such mounds likely consist of a mixture of tar and sediment. Lorenson and others (2014)

structural grain. In the offshore, the fault was difficult to map, despite our dense coverage of seismic-reflection data (see sheet 7), because (1) the pre-LGM section on the shelf includes massive, reflection-free zones, probably caused by either interstitial gas or steeply dipping strata, and (2) the adjacent slope is mainly underlain by the massive to chaotic seismic facies of the Conception fan. The location of the fault on our map coincides with the northwestern margin of the Gaviota sediment bar on the midshelf to outer shelf (see fig. 1–2, in pamphlet; see also, sheets 1, 2), suggesting that faulting may have been a control on bar development. In contrast to previously published offshore mapping of Fischer (1998), we map the Santa Ynez Fault as having a straighter strike (at about 224° azimuth) and being located as much as 900 m farther northwest on the midshelf to outer shelf. Both Fischer (1998) and Eichhubl and others (2002) inferred that the Santa Ynez Fault "captured" the heads of "Drake Canyon" and "Sacate Canyon" at the shelf break; indeed, the linearity of these canyon heads is striking, and it suggests left-lateral slip. Accordingly, our map shows a secondary, discontinuous strand of the fault that extends through these canyon heads; however, we cannot trace these strands to the northeast across the shelf using seismic-reflection profiles, and so their presence is based solely on bathymetry. South of the map area, the south strand of the Santa Ynez Fault appears to disperse into a diffuse zone of several shorter, more east-west-striking contractional faults on the outer shelf, and it cannot be

traced across the slope into deeper water. This fanlike pattern of faults is characteristic of terminating strike-slip faults (Christie-Blick and Biddle, 1985; Mann, 2007). In the offshore part of the map area, closely spaced seismic-reflection profiles (see sheet 7) image many shallow, west-northwest-striking folds that have variable geometries, lengths, amplitudes, degrees of continuity, and wavelengths. The two longest folds, the 17-km-long Molino Anticline and the 22-km-long Government Point Syncline, are truncated to the west and east, respectively, by the south strand of the Santa Ynez Fault. These regionally extensive folds, as well as many other shorter, east-west-striking structures, are probably rooted in blind thrust faults and back-thrust faults in the hanging wall above the Pitas Point–North Channel Fault system.

- REFERENCES CITED Christie-Blick, N., and Biddle, K.T., 1985, Deformation and basin formation along strike-slip faults, in Biddle, K.T., and Christie-Blick, N., eds., Strike-slip deformation, basin formation, and sedimentation: Society of Economic Paleontologists and Mineralogists Special Publication 37, p. 1–34. Dibblee, T.W., Jr., 1988a, Geologic map of the Santa Rosa Hills and Sacate quadrangles, Santa Barbara County, California
- (H.E. Ehrenspeck, ed. [1988]): Dibblee Geological Foundation Map DF-17, scale 1:24,000. Dibblee, T.W., Jr., 1988b, Geologic map of the Solvang and Gaviota quadrangles, Santa Barbara County, California (H.E. Ehrenspeck, ed. [1988]): Dibblee Geological Foundation Map DF-16, scale 1:24,000. Draut, A.E., Hart, P.E., Lorenson, T.D., Ryan, H.F., Wong, F.L., Sliter, R.W., and Conrad, J.E., 2009, Late Pleistocene to Holocene sedimentation and hydrocarbon seeps on the continental shelf of a steep, tectonically active margin, southern California, USA: Marine Geophysical Research, p. 193–206, available at https://doi.org/10.1007/s11001-009-9076-y.
- Eichhubl, P., Greene, H.G., and Maher, N., 2002, Physiography of an active transpressive margin basin—High-resolution bathymetry of the Santa Barbara basin, southern California continental borderland: Marine Geology, v. 184, p. 95–120. Fischer, P.J., 1998, Structure and tectonics of northwestern Santa Barbara basin, *in* Kunitomi, D.S., Hopps, T.E., and Galloway, J.M., eds., Structure and petroleum geology, Santa Barbara Channel, California: American Association of Petroleum Geologists, Pacific Section, and Coast Geological Society, Miscellaneous Publication 46, p, 79–96. Fischer, P.J., and Cherven, B.B., 1998, The Conception Fan, Santa Barbara Basin, California, in Kunitomi, D.S., Hopps, T.E.,
- and Galloway, J.M., eds., Structure and petroleum geology, Santa Barbara Channel, California: American Association of Petroleum Geologists, Pacific Section, and Coast Geological Society, Miscellaneous Publication 46, p, 155–181. Golden, N.E., and Cochrane, G.R., 2013, California Seafloor Mapping Program video and photograph portal: U.S. Geological Survey, Coastal and Marine Geology Program data portal, available at https://doi.org/10.5066/F7J1015K. Keller, E.A., Duffy, M., Kennett, J.P., and Hill, T., 2007, Tectonic geomorphology and hydrocarbon-induced topography of the mid-Channel anticline, Santa Barbara basin, California: Geomorphology, v. 89, p. 274–286. Kunitomi, D.S., Hopps, T.E., and Galloway, J.M., eds., 1998, Structure and petroleum geology, Santa Barbara Channel, California: American Association of Petroleum Geologists, Pacific Section, and Coast Geological Society, Miscellaneous
- Lorenson, T.L., Wong, F.L., Dartnell, P., and Sliter, R.W., 2014, Greenhouse gases generated from the anaerobic biodegradation of natural offshore asphalt seepages in southern California: Geo-Marine Letters, v. 34, p. 281–295, available at https://doi.org/10.1007/s00367-014-0359-1. Mann, P., 2007, Global catalogue, classification, and tectonic origin of restraining and releasing bends on active and ancient
- strike-slip fault systems, in Cunningham, W.D., and Mann, P., eds., Tectonics of strike-slip restraining and releasing bends: London, Geological Society of London, Special Publication 290, p. 13–142. National Geodetic Survey, 2016, NOAA Shoreline Data Explorer: National Oceanic and Atmospheric Administration, National Geodetic Survey data viewer and database, accessed May 1, 2016, at http://www.ngs.noaa.gov/NSDE/. Redin, T., Forman, J., Kamerling, M., and Galloway, J., 2005, Santa Barbara Channel structure and correlation sections—CS-32 to CS-42: American Association of Petroleum Geologists, Pacific Section, Publication CS 36, 12
- Reid, J.A., Reid, J.M., Jenkins, C.J., Zimmerman, M., Williams, S.J., and Field, M.E., 2006, usSEABED—Pacific Coast (California, Oregon, Washington) offshore surficial-sediment data release: U.S. Geological Survey Data Series 182, available at http://pubs.usgs.gov/ds/2006/182/. Sorlien, C.C., and Nicholson, C., 2015, Post 1-Ma deformation history of the Pitas Point-North Channel-Red Mountain fault system and associated folds in Santa Barbara channel, California: U.S. Geological Survey National Earthquake Hazards
- Reduction Program final report, Award G14AP00012, 24 p., available at https://earthquake.usgs.gov/cfusion/ Steel, E., Simms, A., Warrick, J., and Yokoyama, Y., 2015, Depositional history and stratigraphic architecture of lofted hyperpycnal flows in the Santa Barbara Channel, southern California [abs.]: American Association of Petroleum
- Geologists, Pacific Section, Convention, Oxnard, Calif., May 3–6, 2015, available at http://www.searchanddiscovery.com/abstracts/html/2015/90215pacsec/abstracts/S02.0.03.html. Warrick, J.A., Simms, A.R., Ritchie, A., Steel, E., Dartnell, P., Conrad, J., and Finlayson, D.P., 2013, Hyperpycnal plume-derived fans in the Santa Barbara Channel, California: Geophysical Research Letters, v. 40, p. 2,081–2,086. Yerkes, R.F., Wagner, H.C., and Yenne, K.A., 1969, Petroleum development in the region of the Santa Barbara Channel: U.S.

Geological Survey Professional Paper 679–B, p. 11–21.









<sup>1</sup>U.S. Geological Survey;

<sup>2</sup>California Geological Survey

ffshore of Gaviota map area, California, *sheet 9 in* Johnson, S.Y., Dartnell, P., Cochrane, G.R., Hartwell, S.R., Golden, N.E., Kvitek, R.G.

and Davenport, C.W. (S.Y. Johnson and S.A. Cochran, eds.), California State Waters Map Series—Offshore of Gaviota, California: U.S.

Geological Survey Open-File Report 2018–1023, pamphlet 41 p., 9 sheets, scale 1:24,000, https://doi.org/10.3133/ofr201810